

Structural, optical and electrical properties of gamma-rays exposed selenium nanowires

Kiran Mohan Chintala¹ · Suresh Panchal¹ · Pallavi Rana¹ · R. P. Chauhan¹

Received: 8 February 2016 / Accepted: 9 April 2016 / Published online: 15 April 2016
© Springer Science+Business Media New York 2016

Abstract The increasing use of semiconducting nanowires in applications that require prolonged exposure to high energy photons (X-rays and gamma rays) necessitates a better understanding of the effects of irradiation on them. In this context, we synthesized selenium nanowires of 80 nm diameter using template assisted electro-deposition technique and exposed them to gamma rays using Co-60 source at Inter University Accelerator Centre, New Delhi, India. The effect of gamma irradiation on their structural, optical and electrical properties was investigated. The analysis of XRD of pre- and post- irradiated Se nanowires showed no shifting in the peak positions. However, Texture analysis demonstrates the variation in the relative intensity with changing preferred orientation at the higher doses. The optical study was done using UV–Vis spectrophotometer and was found that the optical band gap decreased with increasing gamma irradiation dose. Current–Voltage characteristics of pristine and irradiated Se nanowires also exhibit an enhancement in the current with the exposed dose. The decrease in band gap and an increase in current conduction may be attributed to the decrease in scattering of charge carriers from the grain boundaries and creation of more number of electron-hole pairs.

1 Introduction

Nanostructures confined in several dimensions within the nanometric range, display unique and peculiar properties superior to their bulk counterparts. These unique properties can be attributed to the restricted motion of electrons in the confined dimensions of the nanostructures [1]. For practical applications, the deeper understanding of utilization and tailoring of the nanomaterials is an area of research interest. A large variety of nanomaterials have been synthesised and incorporated in devices that demonstrate their potential to significantly enhance the performance of currently used technology [2, 3]. Semiconducting nanowires, where charge carriers flow in one direction, have enormous research interest because of their excellent electrical and optical properties. Semiconducting nanowires possess huge applications in the field of electronics such as field effect transistors, sensors, lasers, solar cells and photo detectors [4, 5]. These nanowires are important because of their ability to miniaturize the device size as well as to enhance the device performance. Among various semiconducting materials, elemental selenium is a p-type semiconductor with a narrow band gap of ~ 1.6 eV, having potential applications in rectifiers, chemical and biological sensors, xerox machines and solar cells [6, 7]. It is a highly reactive material which can form compound materials with great ease. Spectral response of selenium nanowires includes entire range of visible spectrum which is a much needed characteristic of photoconductors.

There are several methods for synthesizing nanowires e.g. hydrothermal method, vapour phase growth, solution phase approach, template based method, etc. [8, 9]. Among these, electro deposition using template based synthesis provides free standing nanowires with controlled length and diameter. The membrane-based approach has an

✉ R. P. Chauhan
chauhanrpc@gmail.com

¹ Department of Physics, National Institute of Technology, Kurukshetra, Kurukshetra, Haryana 136119, India

advantage of the ability to guide the 1D growth of nanostructures through chemical conversion and the solubility of the alumina/polycarbonate membrane in appropriate solvents enables the release of the as-grown nanostructures [10, 11].

Radiation interactions with nanowires grab enormous interest of the researchers. The controlled radiation on the nanowires enables one to enhance their properties to great extent. The study of irradiation on nanowires also provides the information about the device operation in harsh environment as well as in harsh radiation fluxes. The radiation effect on nanostructures is expected to be more (due to their large aspect ratio) than their bulk counterparts. Radiation often modifies the structure and consequently the other physical properties of materials. Therefore, the irradiation process could be counted as a strong criterion to introduce changes in the structural and electrical properties of nanowires. Irradiation on materials shows positive effects, particularly for nanostructured systems under controlled irradiation conditions. In particular, the irradiation of nanowires with gamma rays induces several changes in their structural, electrical and optical properties [12–15]. The structural damages, such as frenkel defects, might be occurring at high radiation fluence.

Recent studies demonstrate the improvement both in young's modulus and electrical conductivity of gamma irradiated carbon nanotubes. It was found that these properties reached maximum at critical dosage value. Also, the functionalization of CNT's can be increased by irradiating them with gamma rays [16]. ZnO is an II–VI semiconductor compound which showed blue-shift in the emission peak after irradiation with gamma rays [17]. Kumari et al. [18] studied the effect of gamma rays on CdSe nanowires and observed an increase in the grain size as well as in the electrical conductivity of nanowires.

In the present study, we synthesized selenium nanowires of 80 nm diameter using template based electro-deposition method and quantitatively analyzed the modifications induced in their electrical and optical properties before and after irradiation with gamma rays at various doses. The physical properties are stated using XRD and SEM analysis.

2 Experimental details

2.1 Synthesis of selenium nanowires

For the synthesis of selenium nanowires Whatman made track etched polycarbonate membranes, having pore diameter of 80 nm and thickness of 10 μm , were used. Before deposition, a thin layer of gold of the order of 25–30 nm was coated on one side of polycarbonate

membrane. A three-electrode set up was used for the electrochemical deposition. The electrolyte used consisted of selenium dioxide and boric acid in de-ionized water. pH of as prepared solution was maintained at 2. The chemicals used for the synthesis of selenium nanowires were of AR grade. Deposition was carried out in a cell made up of Perspex having a hole of diameter of the order of 1 cm at the bottom. Copper tape with coated membrane facing the cell upwards acted as working electrode. A thin platinum wire of diameter of 5 mm was used as counter electrode and a saturated Ag/AgCl was used as a reference electrode. All the potentials were applied with respect to Ag/AgCl reference electrode. The deposition was carried out by using chrono-amperometry at -1 Volt with the help of SP-240 Biologic Potentiostat. The potential was optimized by cyclic voltametry technique. The deposition process was carried out at 30 °C. After the complete deposition of selenium nanowires, the electrolyte from cell was poured off and the sample was carefully detached from the working electrode and dried at room temperature in the open atmosphere.

2.2 Irradiation parameters

As prepared selenium nanowires were exposed to gamma rays at different doses of 50, 100, 150, 200 KGy from Co⁶⁰ source in Gamma chamber 1200 BNT at Inter University Acceleration Centre (IUAC), New Delhi, India. Dose was changed by changing the time of exposure. At the time of exposure, activity of the source was 4.533 KGy/hour.

2.3 Characterizations

The crystal structure of pristine and gamma irradiated selenium nanowires was analyzed by Rigaku Mini-Flex X-Ray diffractometer using CuK α radiation having wavelength (λ) of 1.54 Å. The estimation of crystallite size was made from X-ray broadening by Scherrer method. For the study of optical properties, a double beam UV–visible spectrophotometer was used. Electrical properties of pristine and irradiated nanowires were determined with the help of Keithley 2400 series source meter and a probe station which consisting of two tungsten tips one of which was touched to copper substrate and another one was gently placed on top of the wires embedded within the polycarbonate membrane so that the tip just touched the top of the wires. The morphology of the selenium nanowires was observed by using JEOL JSM-6390LV scanning electron microscope (SEM). For SEM analysis, template was removed with the help of dichloromethane, ethanol and de-ionized water. To remove the template, sample was dipped in the solution of dichloromethane for 8–10 min and then rinsed with ethanol and water. The sample thus

obtained was then dried and coated with gold palladium alloy for SEM analysis.

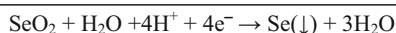
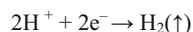
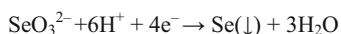
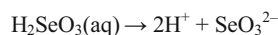
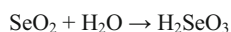
3 Result and discussion

3.1 Selenium nanowires deposition

The deposition of selenium nanowires was done at -1 V by using chronoamperometry (CA) and its current–time ($I-t$) response is shown in Fig. 1. The length of the wires was controlled by optimizing the deposition time.

During the first step of deposition process, SeO_2 gets dissolved in de-ionized water to form selenious acid. In the next step, dissociation of the selenious acid into oxyanion selenite (SeO_3^{2-}) and hydrogen ion (H^+) took place. Third step involves the reduction of selenite ion (SeO_3^{2-}) into solid selenium (Se) at working electrode, on applying voltage and simultaneous reduction of H^+ ion to form hydrogen gas.

The chemical reactions can be summarized as follows:



The consumption of H^+ ions increases the pH level of the solution, which causes the poor filling of pores at bottom. To control the pH level of the solution, boric acid was added which acts as buffer [19].

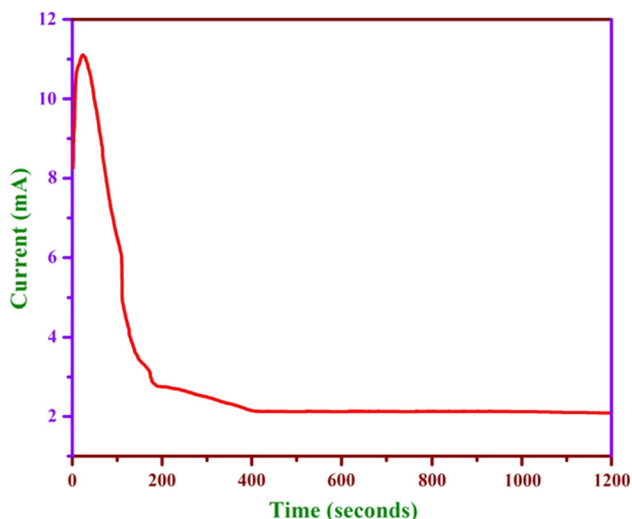


Fig. 1 $I-t$ graph of the selenium nanowires deposition

3.2 Morphological analysis

SEM image of the as prepared selenium nanowire of diameter 80 nm is shown in Fig. 2. The image confirmed the uniform deposition of nanowires in the whole area whose length was found to be of the order of $10\ \mu\text{m}$, which also confirms the complete deposition of nanowires. However, some wires are small in length and not completely vertically aligned, since due to the dissolution some nanowires may break and got tilted.

3.3 Structural analysis

Structural studies were carried out for pristine and gamma irradiated selenium nanowires. Figure 3 depicted the polycrystalline nature of the nanowires as it consists the diffraction peaks of the different families, which were closely matched with JCPDS card 020677. Selenium nanowires persisted the hexagonal structure. Figure 4 shows the diffraction patterns of gamma irradiated selenium that ensured no impurities after the gamma irradiation as no new peak was seen in the patterns. No shifting in 2θ position of the diffraction peaks was observed in spectra that ensures the stability of the hexagonal structure of the irradiated selenium nanowires.

Depending on the experimental conditions, epitaxial single crystalline or textured polycrystalline nanowires can be grown on a substrate or planes could be affected with radiation. Polycrystalline material is an aggregate of large number of crystallites (grains), each having its own shape and orientation in space. Manufacturing process leave the grains in certain preferred orientations, unless the crystal orientation is completely random, polycrystalline material is textured and has some preferred crystallographic orientations [20]. The orientation and number of Miller planes within the nano-crystalline material can

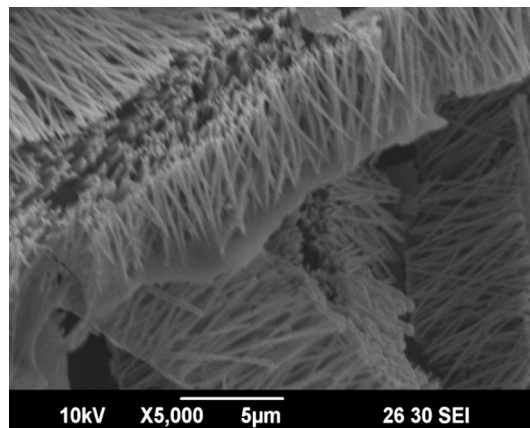


Fig. 2 SEM image of selenium nanowires of 80 nm diameter

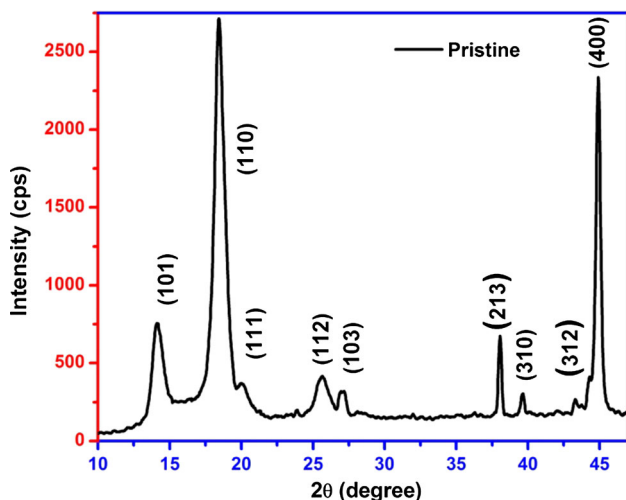


Fig. 3 XRD spectrum of pristine selenium nanowires

also be a platform for device applications such as, monocrystalline nanomaterials are preferred for lasers, solar cells [21, 22].

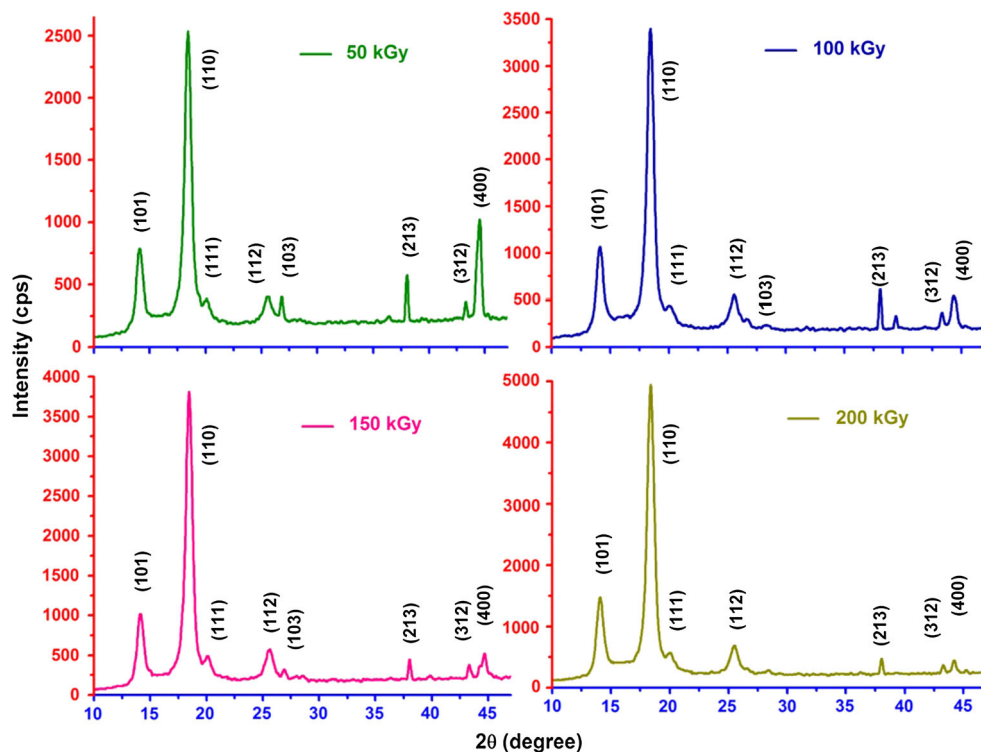
Variation in the peaks intensities is visualized from the XRD spectra of gamma irradiated selenium nanowires. The relative intensity of lines in the diffraction pattern of XRD spectra is affected by: polarization ($1 + \cos^2 2\theta$), structure (F), multiplicity (p), Lorentz, absorption and temperature factor $\{\exp(-2M)\}$ [23] that can be summarized in a following manner;

$$I = F^2 p \left(\frac{1 + \cos^2 2\theta}{\sin^2 \theta \cos \theta} \right) e^{-2M} \quad (1)$$

Absorption factor is independent of θ , so it is not considered here. As ' 2θ ' position of the diffraction peaks was not changed therefore, for this material the structure factor and polarization factor did not affect the intensity. The two possible factors responsible for the variation in intensity of lines may be multiplicity factor (p) and temperature factor. Atoms undergo thermal vibrations and amplification in the amplitude with the increase in the temperature that causes a reduction in the intensities of diffraction lines and a relative increase in the intensity of background scattering between lines. Thus, under these conditions reinforcement of waves scattered at Bragg angles is no longer perfect. Multiplicity factor included all planes for which inter planer spacing is same.

A polycrystalline material also exhibit anisotropy which can be quantified regardless of material anisotropy [24]. The texture of a polycrystal may be quantified by the orientation distribution function. Probability distribution function considering orientation of single crystal as the random variable and equivalently be quantified by texture coefficient (TC). Equation (1) has been derived on the basis of the assumption of random distribution of the specimen's crystals in space. When such type of radical disagreement exists, preferred orientation should be the first possible cause to be suspected. Evaluation of preferred

Fig. 4 XRD spectrum of gamma irradiated selenium nanowires at different doses



orientation can be done on the basis of texture coefficient (TC) [25, 26]:

$$TC = \frac{I(hkl)}{I_0(hkl)} / \frac{1}{n} \sum \frac{I(hkl)}{I_0(hkl)} \quad (2)$$

where $I(hkl)$ stands for measured relative intensity, $I_0(hkl)$ is the relative intensity given in JCPDS card for corresponding peak and n is the number of miller planes. A value of TC greater than 1 indicates the preferred orientation of crystal planes in the given sample and maximum value of TC is given by n (number of miller planes). Values of TC for pristine and gamma irradiated nanowires are summarized in Table 1, wherein TC values in bold italics represents the preferred orientation of the crystal planes.

In the case of pristine nanowires, preferred orientation of the plane {110} and {400} are clearly noticed (Table 1). Texture of the selenium nanowires seems to be affected with exposure of gamma rays with the increase in dose. At higher dose of 200 kGy, texture of crystal plane {400} was shifted towards low value. Overall, it can be concluded from the texture coefficients that crystal plane {110} possess large value after gamma irradiation, while other planes suffers decrement in the values of texture coefficient. This texture variation is also an indication of single-crystallinity of selenium nanowires from polycrystallinity.

Grain size of pre- and post- irradiated samples was determined with the help of Scherrer’s equation;

$$D = (k\lambda) / (\beta \cos \theta) \quad (3)$$

where ‘D’ symbolized for grain size, ‘k’ is scherrer’s constant, also called shape factor, ‘ λ ’ represents the X- ray (CuK_α) wavelength, ‘ β ’ indicates the full width at half maxima (FWHM) in radians and ‘ θ ’ is the Bragg’s angle. The grain size of gamma irradiated nanowires calculated from the Eq. (3) are 18.33, 18.08, 18.35, 19.26 nm for 50, 100, 150 and 200 kGy doses, which are comparable to 17.89 nm for pristine nanowires.

Table 1 Texture coefficient (TC) of pristine and gamma irradiated selenium nanowires

Planes	Pristine	50 kGy	100 kGy	150 kGy	200 kGy
101	0.481	0.663	0.825	0.746	0.754
110	3.517	4.157	5.309	5.377	5.052
111	0.327	0.287	0.328	0.355	0.248
112	0.262	0.212	0.369	0.400	0.330
103	0.274	0.292	0.411	–	–
213	0.603	0.566	0.599	0.332	0.245
310	0.207	–	0.252	–	–
312	0.194	0.262	0.287	0.261	0.154
400	3.146	1.561	0.618	0.365	0.221

3.4 Optical analysis

Optical band gap (E_g) of pristine and gamma irradiated selenium nanowires were calculated using UV–visible spectroscopy. Absorption spectra of the samples were recorded after dissolution of the polycarbonate membrane (Fig. 5). Absorption peak around 580 nm for the pristine nanowires was shifted towards higher wavelength (up to 670 nm) under the influence of gamma exposure. The intensity of the absorption peaks of irradiated nanowires was increased along with the shifting in the absorption edges that depicted the evolution of defects and rise in defect levels. Optical band gap was calculated by tauc plot using absorption spectra of the nanowires.

Tauc and Menth [27] argued that an extrapolation of the nearly linear-functional dependence of $(\alpha h\nu)^n$ allowed an optical energy gap to be defined. Absorption coefficient (α) was determined using law of absorption and mathematically $\alpha = 2.303 (\text{Abs}/t)$, where Abs—Absorbance and t —thickness of the sample (10 μm). The relation $(\alpha h\nu)^n = k (h\nu - E_g)$, pooled the absorption coefficient (α) and optical band gap (E_g). In the relation, k —constant related to effective mass of charge carriers; $h\nu$ —photon energy, n —an index, whose value is 2 (for crystalline semiconductor) [28]. In Tauc plot $(\alpha h\nu)^2/v/s$ hv, intercept of $(\alpha h\nu)^2$ on the energy axis depicted the optical band gap of nanowires. Figure 6 revealed tauc plot of pristine and gamma irradiated selenium wires at different doses.

The optical band gap decreased from ‘2.0 eV’ to ‘1.92 eV’ as the gamma doses changes from dose 50 to 200 kGy while for pristine it is ‘2.01 eV’. When the gamma radiation interacts with the material, two effects will take place at the same time; defect creation and defect annihilation. Perhaps, former effect dominate in our case,

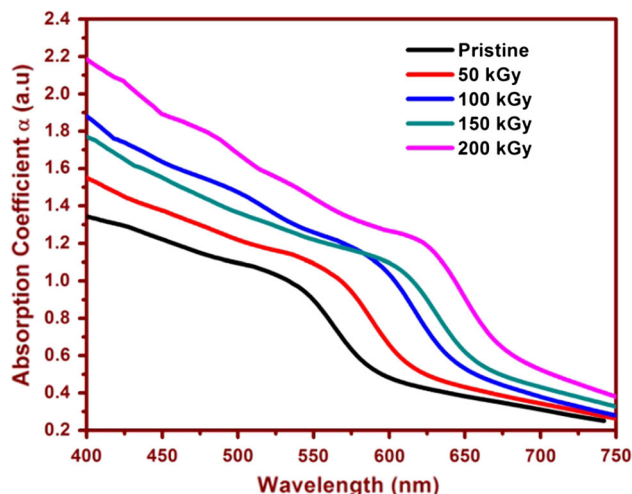


Fig. 5 Absorption plot of pristine and gamma irradiated selenium nanowires

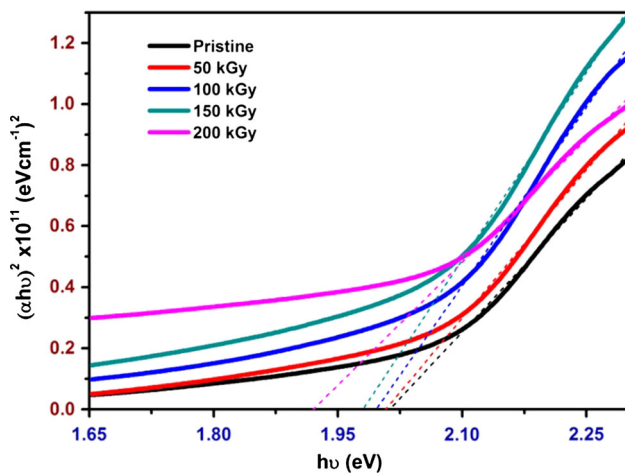


Fig. 6 Tauc plots of pristine and gamma irradiated selenium nanowires

means defects creation take place that affects the corresponding energy width of the bands. As a result, some defects levels and localized states created in the forbidden gap, near the valence and conduction band edges. Therefore, electrons can move to conduction band even at energies below the band gap. Earlier post-irradiation studies also reported reduction in the optical band gap of the nanowires [29–31]. Thus, we can conclude from the optical study that defects are created due to energy imparted by the gamma rays resulting decrement in the optical band gap of selenium nanowires.

3.5 Electrical properties

I–V characteristics of pristine and gamma irradiated selenium nanowires are shown in Fig. 7. All the characteristics were plotted with the help of polynomial fitting of second order for voltage ranging from -1.5 V to $+1.5$ V. For I–V measurements a fine tungsten tip of diameter $10\ \mu\text{m}$ was used which covered around 480 nanowires of diameter $80\ \text{nm}$. Hence, the observed characteristics are the integrated outcome of an array of parallel nanowires.

From the comparative analysis, an increment in the current was depicted with the increase in dose. The incident radiation can change the amplitude of the lattice vibrations, which could be constructive or destructive. The increase in the amplitude of atomic vibrations may depend on the amount of energy transferred by the incident photon to the atom, in addition to the temperature factor. Due to this fractional part of transferred energy, atom may be able to undergo translatory or vibrational motion, and can affect the process of electron scattering and thus may affect the electrical resistivity of nanowires. However, vibrational motion is very less as compared to the translational motion. Hence, one can conclude that the scattering due to lattice

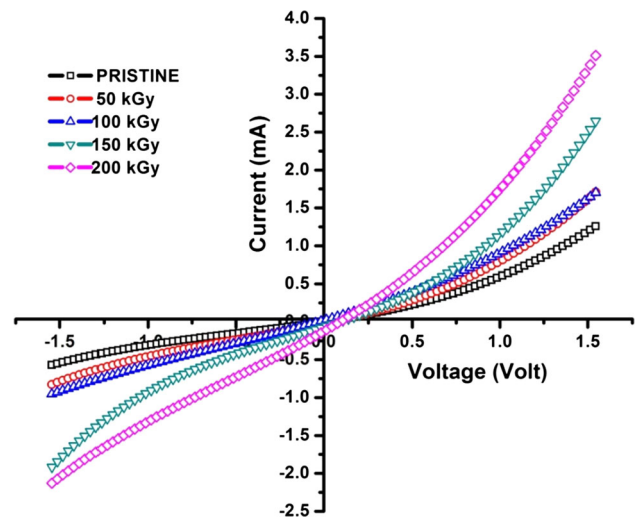


Fig. 7 IVC of pristine and gamma irradiated selenium nanowires at different doses

vibrations contributed from gamma rays may be negligible and thus, net gamma rays irradiation plays an imperative role in the increase of the number of charge carriers.

Energy deposited by gamma rays along their track also leads to creation of defects in the material in the form of vacancies, dislocation etc. [32–34]. Numerous controlled defects such as point cluster and columnar defects were produced in materials due to electronic excitations [35]. In addition, the density of intrinsic charge carriers (electron and hole) is also modified as imparted energy contributing by gamma rays may break the covalent bonds. In semiconductors, gamma rays may provide sufficient energy to the valence electrons to move them into the conduction band and create electron-hole pairs. Excitation of valence electrons into the conduction band can significantly increase the electrical conductivity of nanowires that in well conformity with the optical studies of the nanowires, discussed in earlier section. Additionally, enhancement in density of the charge carriers also stimulates the reduction in the number of defects in the inter- and intra-grain regions. An increased density of donors can reduce the height of the potential barrier, resulting in less diffusive scattering of the charge carriers from the grain boundaries and increasing the electrical conductivity of the nanowires. Moreover, randomly distributed grain boundaries regarded as potential barriers that reflected a fraction of the charge carriers. These boundaries act as partially reflecting surfaces perpendicular to the direction of the electric field in a material, providing additional scattering sites, and they have been found to be affected by the orientation of the grains. Movement of grain boundaries requires less activation energy compared with other defects. When we concentrate on the movement of the crystal planes,

considerable variation was observed in the orientation of the crystal planes with gamma doses (Table 1). Hence, gamma irradiation influenced the scattering of charge carriers from the grain boundaries with a positive approach and supported the enhancement in the current through the irradiated nanowires.

4 Conclusions

From the gamma irradiation on selenium nanowires it may be concluded that radiation should not always be viewed on negative side, however the limit of its usefulness is a hard step to define, but it can also be considered as a tool to solve physical problems. The electrical transportation in the selenium nanowires got sufficiently enhanced after the gamma irradiation without any transformation in the basic crystal structure (hexagonal) of nanowires. In addition, the plane orientation i.e. texture coefficient also indicated the variation in the crystallinity of nanowires from polycrystalline to single-crystalline. Present study might have prepared a strong background from application point of view to utilize the radiation modified electrical conductivity as ground for device fabrication.

Acknowledgments The authors are thankful to IUAC New Delhi, India for providing Gamma source for irradiation of our samples. The financial support in form of the project no. IUAC/XIII.7/UFR-56303 is also thankfully acknowledged.

References

1. E. Roduner, Chem. Soc. Rev. **35**(7), 583 (2006)
2. D. Rawtani, T. Sajan, R. Amipara Twinkle, Y.K. Agrawal, Rev. Adv. Mater. Sci **40**, 177 (2015)
3. D.Y. Jeon, S. Pregl, S.J. Park, L. Baraban, G. Cuniberti, T. Mikolajick, W.M. Weber, Nano Lett. **15**(7), 4578 (2015)
4. M.H. Huang, S. Mao, H. Feick, H. Yan, Y. Wu, H. Kind, E. Weber, R. Russo, P. Yang, Science **292**(5523), 1897 (2001)
5. B. Tian, X. Zheng, T.J. Kempa, Y. Fang, N. Yu, G. Yu, J. Huang, C.M. Lieber, Nature **449**(7164), 885 (2007)
6. D. Qin, H. Tao, Y. Zhao, L. Lan, K. Chan, Y. Cao, Nanotechnology **19**(35), 355201 (2008)
7. S.Y. Lee, T.H. Kim, D.I. Suh, E.K. Suh, N.K. Cho, W.K. Seong, S.K. Lee, S.K. Appl. Phys. A **87**(4), 739 (2007)
8. S.N. Bai, S.C. Wu, J. Mater. Sci.: Mater. Electron. **22**(4), 339 (2011)
9. H.M. Shang, C. Guozhong, Template-based synthesis of nanorod or nanowire arrays, In Springer Handbook of Nanotechnology, Springer Berlin Heidelberg, 169 (2010)
10. S. Kumar, J. Exp. Nanosci. **4**(4), 341 (2009)
11. X.Y. Zhang, Y. Cai, J.Y. Miao, K.Y. Ng, Y.F. Chan, X.X. Zhang, N. Wang, J. Crys. Growth **276**(3), 674 (2005)
12. P. Rana, R.P. Chauhan, Phys. B Condens. Matter **451**, 26 (2014)
13. D. Nikolić, V. Aleksandra, FME Trans. **44**, 99 (2016)
14. M.M. Mutter, H.K. Atty, A.A. Hateef, Inter. Lett. Chem. Phys. Astrol. **63**, 22 (2016)
15. A.M. Abdelghany, E.M. Abdelrazek, S.I. Badr, M.A. Morsi, Mater. Des. **97**, 532 (2016)
16. B.I. Kharisov, O.V. Kharissova, U.O. Méndez, *Radiation Synthesis of Materials and Compounds* (CRC Press, 2013)
17. M.J.F. Empizo, K. Yamanoi, K. Mori, R. Arita, K. Iwano, M. Takabatake, K. Fukuda, T. Hori, Y. Minami, M.V. Luong, Y. Abe, Appl. Phys. Exp. **8**(6), 061101 (2015)
18. M. Kumari, P. Rana, R.P. Chauhan, Nucl. Instrum. Methods A **753**, 116 (2014)
19. N. Kumar, R. Kumar, S. Kumar, S.K. Chakarvarti, J. Mater. Sci. Mater. Electron. **25**(8), 3537 (2014)
20. R. Paroni, J. Elast. **60**, 19 (2000)
21. S.P. Harimkar, N.B. Dahotre, J. Appl. Phys. **100**, 024901 (2006)
22. M.D. Sabatino, M. Juel, L. Arnberg, M. Syvertsen, G. Tranell, Control of grain size and orientation in multi-crystalline silicon ingots. Trans. Indian Inst. Met. **62**(4–5), 511 (2009)
23. B.D. Cullity, in Elements of X-Ray Diffraction, ed. by M.Cohen (Addison-Wesley publishing company Inc., Massachusetts, 1978)
24. J.C. Nadeau, M. Ferrari, Int. J. Solids Struct **38**, 7945 (2001)
25. C. Barret, T.B. Massalski, *Structure of Metals: Crystallographic Methods, Principles and Data*, 3rd edn. (University of Michigan, Pergamon press, Oxford, 1980)
26. G.B. Harris, Philos. Mag. **43**, 133 (1952)
27. J. Tauc, A. Menth, J. Non-Cryst. Solids **8**, 569 (1972)
28. S.C. Singh, K.R. Swarnkar, R. Gopal, Bull. Mater. Sci. **33**, 21 (2010)
29. A. M. S. Galante, L. L. Campos, Characterization of polycarbonate dosimeter for gamma-radiation dosimetry. In Proceedings of Third European IPRA Congress, Helsinki, Finland, 2010
30. R.P. Chauhan, D. Gehlawat, A. Kaur, J. Exp. Nanosci. **9**(8), 871 (2012)
31. P. Rana, R.P. Chauhan, J. Mater. Sci. Mater. Electron. **25**, 5630 (2014)
32. L. Van, A.J. Victor, Nucl. Instrum. Methods A **25**(3), 453 (1987)
33. S.T. Lai, D. Alexiev, B.D. Nener, J. Appl. Phys. **78**(6), 3686 (1995)
34. M. McPherson, B.K. Jones, T. Sloan, Semi. Sci. Technol. **12**(10), 1187 (1997)
35. M. Toulemonde, Nucl. Instrum. Methods B **156**(1), 1 (1999)